^{6}Li NMR Studies of Cation Disorder and Transition Metal Ordering in $Li[Ni_{1/3}Mn_{1/3}Co_{1/3}]O_2$ Using Ultrafast Magic Angle Spinning

L. S. Cahill,[†] S.-C. Yin,[‡] A. Samoson,[§] I. Heinmaa,[§] L. F. Nazar,[‡] and G. R. Goward*[,†]

Department of Chemistry and Brockhouse Institute for Materials Research, McMaster University, 1280 Main Street West, Hamilton, Ontario, L8S 4M1 Canada, Department of Chemistry, University of Waterloo, Waterloo, Ontario, Canada, and National Institute of Chemical Physics and BioPhysics, Tallinn, Estonia

Received April 25, 2005. Revised Manuscript Received October 13, 2005

Studies of $Li[Ni_{1/3}Mn_{1/3}Co_{1/3}]O_2$ prepared under six different conditions are compared using high-resolution solid-state ^{6}Li NMR. Differing degrees of cation disorder are established via integration of the NMR resonances, and this quantification of cation disorder is compared with Rietveld refinements of powder X-ray and neutron diffraction studies. Chemical shift trends to high frequency with decreasing degrees of disorder are established among this family of samples and explained according to the orbital overlap experienced by Li nuclei in the two environments: within the lithium layers and exchanged with nickel into the transition metal layers. Finally, an interesting case of local transition metal charge ordering is observed. Three unique environments are described, which can be accounted for based on electroneutrality arguments, and the known clustering of Ni^{2+} and Mn^{4+}. This effect has not been detected in these materials by other methods including neutron and X-ray diffraction. Thus, the local ordering, which is observed in the dominant NMR resonance of Li in its own layers is thought to be pervasive (affecting the majority of the NMR nuclei), but very local, so as to be seen only by techniques such as NMR which probe immediate neighborhoods.

Introduction

The success of the layered $LiCoO_2$ cathode coupled with a carbonaceous anode has advanced lithium-ion rechargeable batteries to a new era.[1,2] However, the high cost of cobalt has driven research to replace it, in whole or in part, with transition metals such as Ni and Mn to meet future demands for large-scale rechargeable batteries. In this paper we explore ordering in $Li[Ni_{1/3}Mn_{1/3}Co_{1/3}]O_2$ which crystallizes in the ordered rock salt α-$NaFeO_2$-type structure ($R\bar{3}m$), isostructural with $LiCoO_2$. This compound has been suggested as a possible cathode material to combine some of the benefits of using Ni (high capacity), Mn (low cost), and Co (stability). $Li[Ni_{1/3}Mn_{1/3}Co_{1/3}]O_2$ has been reported by Ohzuku et al. to have capacities of up to 190−220 mA h g^{-1}.[3] This material is also promising for battery applications because it has been shown to have better thermal stability than $LiCoO_2$.[4]

Structural properties are related to the electrochemical performance of cathode materials. The understanding of lithium location and transport within the lattice is essential to design concepts that will lead to the development of new materials. ^{7}Li/ ^{6}Li solid-state NMR is an effective technique to study these microscopic processes, especially when coupled with X-ray diffraction that gives long-range structural information. Layered cathode materials such as $Li[Ni_{1/2}Mn_{1/2}]O_2$ and, to a lesser extent, $Li[Ni_{1/3}Mn_{1/3}Co_{1/3}]O_2$ undergo mixing of lithium in the lithium layer and nickel from the transition metal layers because of their similar cationic radii ($Li^+ = 0.76$ Å, $Ni^{2+} = 0.69$ Å). This cation disorder has been shown to be correlated to irreversible capacity, possibly because it impedes lithium diffusion.[5] By comparing the area ratios of the (003) and (104) reflections in the X-ray powder diffraction patterns, or by performing quantitative Rietveld analysis, the degree of disorder can be determined experimentally.[6] Solid-state ^{6}Li NMR has also been used in studies of the $Li[Ni_{1/3}Mn_{1/3}Co_{1/3}]O_2$ and $Li[Ni_{1/2}Mn_{1/2}]O_2$ compounds, for the identification of two lithium environments: Li in the lithium oxide layer and Li exchanged with nickel ions in the transition metal layer.[7−10] These previous studies identified the two environments according to their chemical shifts. However, no analysis to ascertain the varying degrees of disorder among materials prepared under different conditions was provided. In this paper we demonstrate the use of solid-state NMR to quantify the degree of cation disorder in $Li[Ni_{1/3}Mn_{1/3}Co_{1/3}]O_2$ samples prepared by a variety of methods. We compare the NMR

* Corresponding author. E-mail: goward@mcmaster.ca. Phone: (905) 525-9140 ext. 24176. Fax: (905) 522-2509.
[†] McMaster University.
[‡] University of Waterloo.
[§] Institute for Chemical Physics and BioPhysics.

(1) Tarascon, J. M.; Armand, M. *Nature* **2001**, *414*, 359−367.
(2) Nagaura, T.; Tozawa, K. *Prog. Batteries Solar Cells* **1990**, *9*, 209−217.
(3) Ohzuku, T.; Makimura, Y. *Chem. Lett.* **2001**, 642−643.
(4) Yabuuchi, N.; Ohzuku, T. *J. Power Sources* **2003**, *119*, 171−174.
(5) Jouanneau, S.; Eberman, K. W.; Krause, L. J.; Dahn, J. R. *J. Electrochem. Soc.* **2003**, *150*, A1637−A1642.
(6) Ohzuku, T.; Ueda, A.; Nagayama, M.; Iwakoshi, Y.; Komori, H. *Electrochim. Acta* **1993**, *38*, 1159−1167.
(7) Yoon, W. S.; Grey, C. P.; Balasubramanian, M.; Yang, X. Q.; Fischer, D. A.; McBreen, J. *Electrochem. Solid State Lett.* **2004**, *7*, A53−A55.
(8) Yoon, W. S.; Paik, Y.; Yang, X. Q.; Balasubramanian, M.; McBreen, J.; Grey, C. P. *Electrochem. Solid State Lett.* **2002**, *5*, A263−A266.
(9) Yoon, W. S.; Iannopollo, S.; Grey, C. P.; Carlier, D.; Gorman, J.; Reed, J.; Ceder, G. *Electrochem. Solid State Lett.* **2004**, *7*, A167−A171.
(10) Grey, C. P.; Yoon, W. S.; Reed, J.; Ceder, G. *Electrochem. Solid State Lett.* **2004**, *7*, A290−A293.

10.1021/cm0508773 CCC: $30.25
Published on Web 11/22/2005

data with neutron and X-ray diffraction studies of the same materials. We extend the investigation to include both quantification of cation disorder and comparison of chemical shift trends among samples with differing degrees of disorder. Solid-state NMR is an extremely valuable technique for elucidating local ordering that may not be revealed by other techniques. Evidence for charge ordering of the transition metals within several of the samples is provided and used to develop a local picture of the lithium environment. Here it is useful to point out that two types of order/disorder are discussed in the paper, the first being the disordering among Ni^{2+} and Li^{+} ions which exchange places with each other in the layered structure, termed *cation disorder*, and the second is ordering of the transition metal ions within their layers to form locally ordered domains, in accordance with the known Ni^{2+}–Mn^{4+} association, predicted in related structures.[9,11] The latter is termed here *transition metal ordering*, for clarity.

Experimental Section

Layered $Li[Ni_{1/3}Mn_{1/3}Co_{1/3}]O_2$ compounds were prepared by the mixed hydroxide method. Stoichiometric amounts of $Co(NO_3)_2\_6H_2O$ (Fisher), $Ni(NO_3)_2\_6H_2O$ (Alfa), and $Mn(NO_3)_2$ (Fisher, 50% Solution) were mixed in deionized water and added dropwise into a 1 M LiOH solution. The resultant precipitates were dried at 150 °C overnight prior to mixing with a stoichiometric amount of $LiOH\_H_2O$ for samples (a) and (b) and 6-Li enriched Li_2CO_3 to provide ^{6}Li enrichment for (c), (d), (e), and (f). The samples were fired at 1000°C for (a), (b), and (c) 3 h and quenched and (d) 12 h and slow-cooled. Samples (e) and (f) were heated to 1100 °C for 3 h and quenched.

^{6}Li NMR spectra were acquired at a Larmor frequency of 29.7 MHz on a 4.7 T magnet, using a probe fitted to support 1.8 mm diameter rotors, spinning at frequencies up to 50 kHz. The spectra were referenced to 1 M LiCl, at 0 ppm. Spectra were acquired using a Hahn-echo pulse sequence, with a 1.7 μs $\pi/2$ pulse, and 3.4 μs π pulse, using an echo delay of two rotor periods, and a recycle delay of 500 ms. For all samples overnight acquisitions of roughly 50k transients were obtained.

^{6}Li spectral decompositions were performed using the xedplot program in the Bruker XwinNMR software. This allows variation of peak position, peak height, line width, and the ratio of Gaussian to Lorentzian functions. 100% Gaussian line shapes were used, as this simplifies the comparison of relative intensities. Error estimates were based on comparisons of multiple deconvolution iterations, which resulted in small variances in peak width and position.

Samples for powder X-ray diffraction (XRD) were measured on a Bruker D8 Advance powder diffractometer using standard Bragg–Brentano geometry with Cu Kα radiation (λ = 1.5406 Å). Data were collected from 10° to 105° in 2θ, using a step size of 0.02° and a count time of 10 s. For powder neutron diffraction (PND) experiments, 2 g of material was loaded in a vanadium can in an Ar-filled glovebox. Patterns were collected over a 16 h period on the C2 constant wavelength (λ = 1.32778 Å) powder diffractometer at Chalk River Laboratories, Canada, in conventional Debye–Scherrer mode. Si powder (NIST 640c) was used as an external calibration standard in a vanadium can and measured in the same configuration as the sample. Measurements were carried out from 5° to 115° in 2θ at 300 K, using a step size of 0.1°. Powder neutron and/or X-ray data sets were both refined by Rietveld methods using the GSAS package with the EXPGUI interface.[12] Backgound, scale factor, zero point, lattice parameters, atomic positions, and coefficients for the peak shape function were iteratively refined until convergence was achieved.

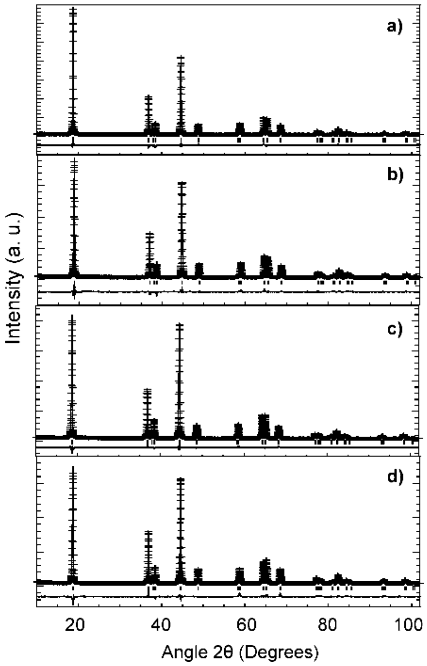

Figure 1. Rietveld refinements of powder X-ray patterns of samples (a)–(d) of $LiCo_{1/3}Ni_{1/3}Mn_{1/3}O_2$. The experimental (+) and calculated (−) data are shown, along with the residual at the bottom of each plot. The positions for the transition metal atoms Co, Ni, and Mn were fixed at the Wyckoff position 3(a) in the unit cell, Li at 3(b), and O at 6(c). Atomic displacement parameters, the fractional coordinate z for O, and the site occupancy exchange of Ni and Li between sites 3a and 3b were refined in all cases, the latter giving rise to values of (a) 2.7%, (b) 3.3%, (c) 7.3%, and (d) 5.5%.

Table 1. Summary of Rietveld Refinements of X-ray Diffraction Data for $Li[Ni_{1/3}Mn_{1/3}Co_{1/3}]O_2$ Samples (a)–(d)

sample	a (Å)	c (Å)	V (Å^3)	R_{wp} (%)	R_B (%)	χ^2
(a)	2.85986(2)	14.2293(2)	100.787(2)	5.32	4.45	2.031
(b)	2.85374(3)	14.2104(3)	100.223(3)	6.3	6.73	2.388
(c)	2.86729(2)	14.2600(2)	101.530(2)	3.79	2.85	2.178
(d)	2.86355(4)	14.2492(3)	101.188(4)	6.39	7.13	2.545

Results and Discussion

The X-ray powder diffraction patterns of four $Li[Ni_{1/3}Mn_{1/3}Co_{1/3}]O_2$ samples prepared under different conditions are shown in Figure 1. Samples (a) and (b) were prepared by reacting natural abundance $LiOH\_H_2O$ with the mixed hydroxides at 1000 °C for 3 h and quenching the oxide. Samples (c) and (d) were prepared similarly but using 6-Li enriched Li_2CO_3 instead of $LiOH\_H_2O$, and sample (d) was slow-cooled rather than being quenched. All patterns were indexed in the space group $R3m$, and refined using the Rietveld method to yield the lattice parameters listed in Table 1 (crystallographic positions for Co, Ni, Mn, Li, and O were typical of those previously described in other publications: see figure caption for details). Refinement in space groups lower than $R\bar{3}m$ such as $P3_112$ did not improve the goodness of fit significantly from a statistical point of view for any of

(11) Meng, Y. S.; Ceder, G.; Grey, C. P.; Yoon, W. S.; Shao-Horn, Y. *Electrochem. Solid State Lett.* **2004**, *7*, A155–A158.

(12) Toby, B. H. *EXPGUI*, a graphical user interface for *GSAS. J. Appl. Crystallogr.* **2001**, *34*, 210–213.

Table 2. Results of Line shape Decomposition for ^{6}Li NMR Spectra of Li[$Ni_{1/3}Mn_{1/3}Co_{1/3}$]O_2 Samples (a)−(d); Comparisons of the Degree of Disorder Determined by NMR, from Integration of the Resonances, to Degree of Disorder Determined from Rietveld Analysis[a]

sample preparation	chemical shift (ppm)	line width (kHz)	% Li/Ni disorder by NMR	% Li/Ni disorder by XRD	% Li/Ni disorder by PND
(a) heated 3 h, 1000 °C, quenched (^{7}Li)	506	20.0	2.5	2.7	3.0
	1283	7.6			
(b) heated 3 h, 1000 °C, quenched (^{7}Li)	483	19.4	3.6	3.3	
	1259	7.8			
(c) heated 3 h, 1000 °C, quenched (^{6}Li)	470	17.5	4.5	7.3	
	1240	13.3			
(d) heated 12 h, 1000 °C, slow-cooled (^{6}Li)	519	19.4	2.3	5.5	
	1280	6.7			

[a] Error estimates are ±10 ppm in the chemical shift and ±0.2 kHz in line width.

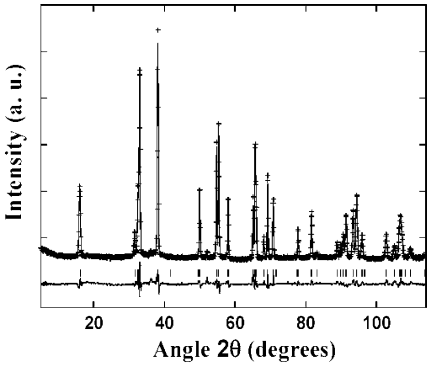

Figure 2. Neutron diffraction pattern of sample (a) of $LiCo_{1/3}Ni_{1/3}Mn_{1/3}O_2$ and Rietveld refinement using the combined X-ray and neutron data. The experimental (+) and calculated (−) data are shown, along with the residual. The positions for the transition metal atoms Co, Ni, and Mn were fixed at the Wyckoff position 3(a) in the unit cell, Li at 3(b), and O at 6(c). Atomic displacement parameters, the fractional coordinate *z* for O, and the site occupancy exchange of Ni and Li between sites 3a and 3b were refined, the latter giving rise to values of 2.9% for the combined XRD and neutron refinement and 3.0% for the neutron refinement alone. The refinement parameters include $a = 2.8597(0)$ Å, $c = 14.227(0)$ Å, $R_{wp} = 4.23\%$, $R_B = 13.89\%$, $\chi^2 = 4.329$.

the materials. This takes into account that the greater number of variables in a refinement in a lower symmetry space group will always produce a slightly better reliability factor R_{wp}. It makes it a poor indicator of the optimum space group unless the difference in the reliability factors is large, which it was not for our materials. The degree of Li/Ni exchange (Table 2) was lowest for samples (a) and (b) prepared from $LiOH\_H_2O$, namely, about 3.0%. This was confirmed for sample (a) by separately carrying out Rietveld refinement on its neutron diffraction pattern (Figure 2; Table 2). Fits using the neutron data alone, and fits using combined XRD and neutron data, yielded essentially the same value of close to 3.0% for the Li/Ni disorder. The PND pattern also showed no evidence of superstructure reflections arising from long-range order, suggesting that the space group $R\bar{3}m$ is the most appropriate choice for describing the bulk properties of our materials. The degree of cation disorder in these materials is discussed below in the context of using NMR as a probe of local order.

Probing the Degree of Cation Disorder by NMR. Lithium NMR spectra are strongly affected by the electronic structure of the local environment within the material. They exhibit a wide range of hyperfine chemical shifts because of the Fermi-contact mechanism: the transfer of unpaired electron spin density from the paramagnetic ions to the Li nucleus. The Fermi-contact shift is additive with a magnitude dependent on the number of d electrons as well as the Li−O−M bond lengths and bond angles within the lattice. Specific hyperfine shifts have been assigned to specific lithium environments within transition metal oxides as shown in the seminal work of Grey et al. on lithium manganates.[13−18] These shifts are based on two possible mechanisms of interaction between the unpaired electrons and the lithium nuclei.[19] The first case is delocalization, which results in the positive transfer of spin density to the lithium nucleus via the oxygen 2p orbital. The second possible transfer is through spin polarization, which results in negative spin density induced on the lithium 2s orbital. Which of these two mechanisms are active depends on the local geometry of the M−O−Li interaction and the electronic structure of the transition metal ion. In general, delocalization is dominant.[19] In Li[$Ni_{1/3}Mn_{1/3}Co_{1/3}$]O_2, Co^{3+} is diamagnetic (low spin $t_{2g}^6e_g^0$) so it does not contribute spin density to the hyperfine shift. Ni^{2+} ($t_{2g}^6e_g^2$) and Mn^{4+} (high spin $t_{2g}^3e_g^0$) both contribute to the observed hyperfine shifts.

Figure 3a,b shows natural abundance ^{6}Li spectra (MAS = 46 kHz) of Li[$Ni_{1/3}Mn_{1/3}Co_{1/3}$]O_2 samples. Spectra for the ^{6}Li-enriched samples are shown in Figure 3c,d. In these materials, the oxidation states of the three transition metals have been previously determined to be Ni^{2+}, Co^{3+}, and Mn^{4+} by density of states calculations and XANES (X-ray absorption near edge spectroscopy) data.[20] In all four spectra, two groups of resonances are evident with large positive shifts due to the Fermi−contact interaction between the lithium nuclear spins and the unpaired electrons of the Ni^{2+}/Mn^{4+} ions. The set of resonances at lower frequency correspond to the Li present in the Li oxide layers, while those at higher frequency are assigned to Li located in the transition metal layers. The presence of Li in the transition metal layer occurs as a result of mixing with the similar-sized Ni^{2+} ions. The results of spectral decomposition performed to fit the line shapes are shown below the experimental data in Figure 3. When the area of the smaller peak is compared to that of the larger peak (including its sidebands), the amount of cation

(13) Lee, Y. J.; Wang, F.; Grey, C. P. *J. Am. Chem. Soc.* **1998**, *120*, 12601−12613.
(14) Lee, Y. J.; Grey, C. P. *Chem. Mater.* **2000**, *12*, 3871−3878.
(15) Pan, C. J.; Lee, Y. J.; Ammundsen, B.; Grey, C. P. *Chem. Mater.* **2002**, *14*, 2289−2299.
(16) Lee, Y. J.; Eng, C.; Grey, G. P. *J. Electrochem. Soc.* **2001**, *148*, A249−A257.
(17) Grey, C. P.; Lee, Y. J. *Solid State Sci.* **2003**, *5*, 883−894.
(18) Grey, C. P.; Dupre, N. *Chem. Rev.* **2004**, *104*, 4493−4512.
(19) Carlier, D.; Menetrier, M.; Grey, C. P.; Delmas, C.; Ceder, G. *Phys. Rev. B* **2003**, *67*, 174103/1−174103/14.
(20) Hwang, B. J.; Tsai, Y. W.; Carlier, D.; Ceder, G. *Chem. Mater.* **2003**, *15*, 3676−3682.

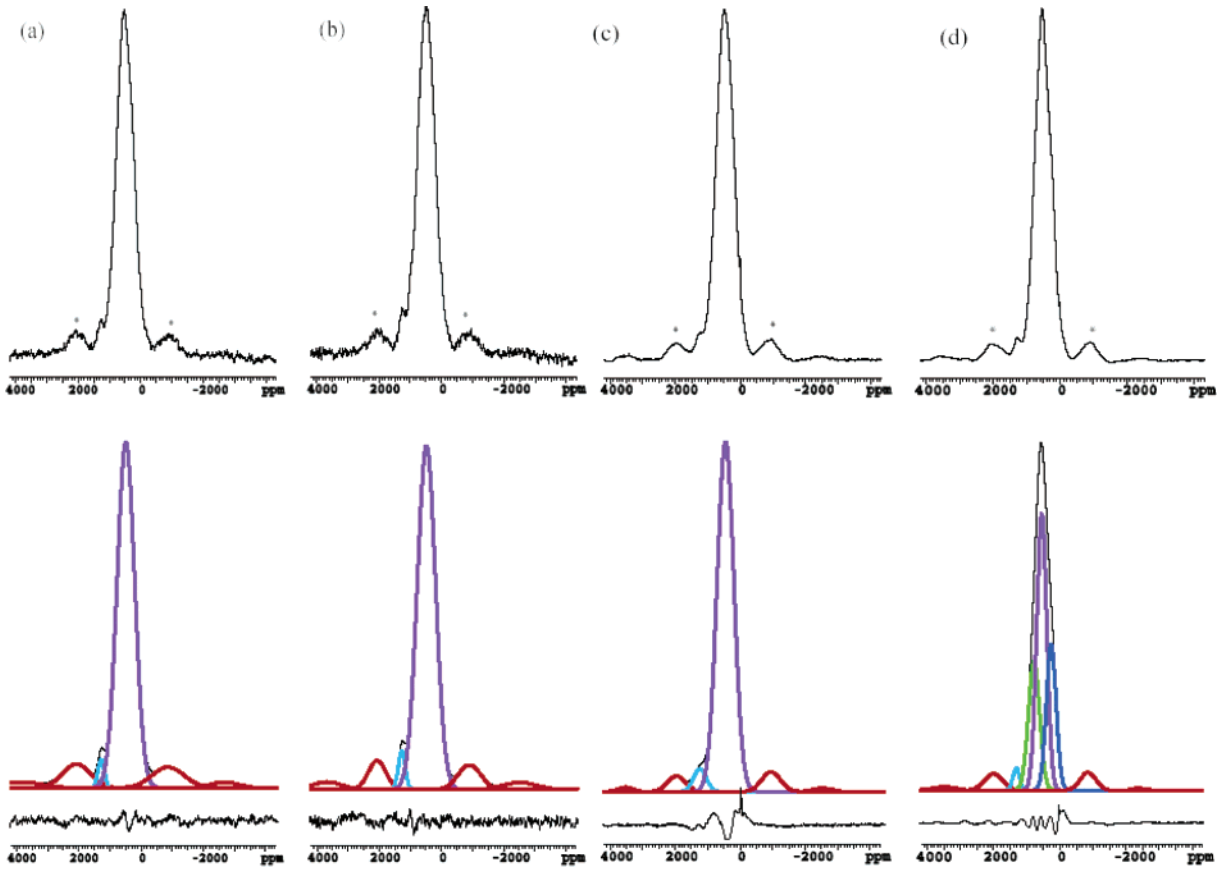

Figure 3. ^{6}Li MAS NMR spectra acquired at 29.7 MHz (4.7 T), under 46 kHz rotor spinning frequencies, in 1.8 mm rotors containing ~5 mg samples (a), (b), and (c) heated for 3 h and quenched from 1000 °C; (d) heated for 12 h and slow-cooled from 1000 °C. The spinning sidebands are marked with asterisk and the spectral decompositions are shown below the experimental data, with the fit in black. The residual difference between the fit and the experimental data is shown below the fit. Error estimates are based on the difference in peak area between repeated iterations of the deconvolution routine.

mixing (degree of cation disorder) can be determined. The cation disorder was determined to be 2.5% and 3.6% for the first two samples, which is in good agreement with the values determined by Rietveld analysis of the X-ray powder diffraction patterns for samples (a) and (b), of 2.7% and 3.3%, respectively. Analysis of the neutron diffraction pattern of sample (a) gave essentially identical results (3.0%; Table 2). The cation disorder for samples (c) and (d) were 4.5% and 2.3%, respectively. These cation disorder values are lower than those obtained from diffraction (7.3% and 5%), although the trend is consistent between these two materials. In both measurements, the highest degree of cation disorder is found for sample (c). The anomaly in the trend among the four samples found for sample (d) is attributed to local transition metal charge ordering, an effect which is not observed in the diffraction studies. The error bars for the chemical shift range and the line shapes broadened by paramagnetic interactions are about 10 ppm for the hyperfine shifts and 0.2 kHz for the line widths. This gives an error of about ±0.1% for the degree of disorder. A summary of the chemical shifts and line widths is given in Table 2.

Correlations between Cation Disorder and Chemical Shifts. The results in Table 2 show an important trend. Samples which exhibit lower cation disorder have greater hyperfine shifts for both sets of resonances; this is most apparent in the high-frequency resonance of the lithium ions in the transition metal layer. It can be explained according to the model for the transfer of spin density as described above for Fermi−contact shift interactions and depicted in Figure 4.[7−9,15,17,19] In the case of the lowest disorder, we expect a strong driving force for the association of Mn^{4+} near the Li^+ in the transition metal layer, driven by Coulombic forces.[8] In the first coordination sphere of lithium,

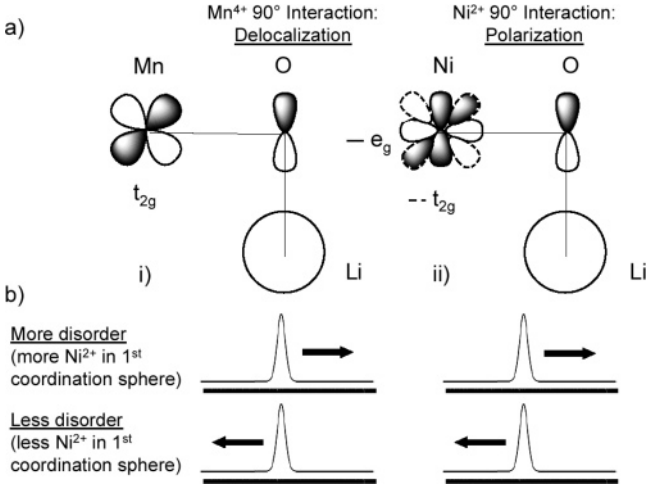

Figure 4. (a) A diagram representing how spin density is transferred from the paramagnetic center of the transition metal ions to the 2s orbital of the Li^+ nucleus via the intervening oxygen orbitals. (i) A 90° Li−O−Mn^{4+} interaction transferring positive spin density by delocalization and (ii) a 90° Li−O−Ni^{2+} interaction transferring negative spin density by polarization. (b) Application of this model to explain NMR results obtained for materials such as Li[$Ni_{1/3}Mn_{1/3}Co_{1/3}$]O_2, in which cation mixing of Li^+ and Ni^{2+} occurs.

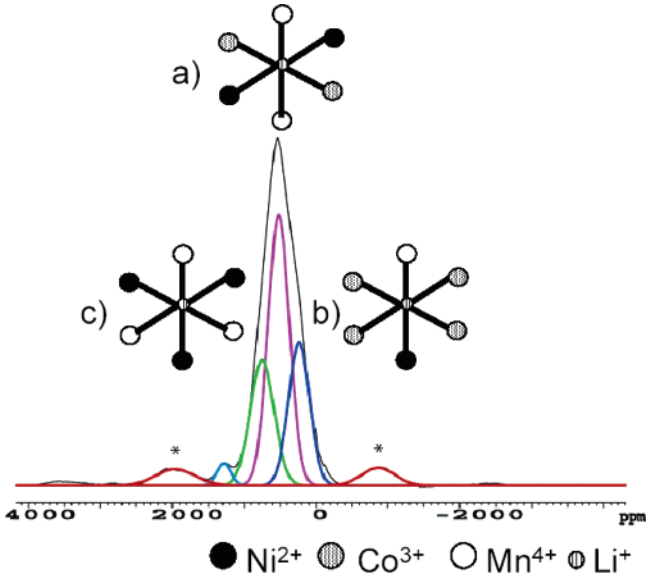

Figure 5. (a) Spectral decomposition of sample (d). The spinning sidebands are marked with asterisk. (b) Proposed coordination environments for three types of observed ^{6}Li resonances in the main line shape, attributable to local charge ordering.

Mn^{4+} will interact with Li via a 90° delocalization of the t_{2g} orbitals with the Li 2s orbital via the oxygen 2p orbital. The delocalization mechanism provides a positive spin transfer; thus, the highest shift is expected for the largest amount of Mn^{4+} in the first coordination sphere. Larger degrees of disorder will interfere with the ordering of Mn^{4+} and Li^+, allowing cobalt or nickel ions into this first coordination sphere. Ni^{2+} ions cannot interact with lithium in the transition metal layer via delocalization, due to the lack of a 90° orbital overlap, so the contribution to the chemical shift is a negative spin transfer occurring via polarization of the lithium 2s orbital by the Ni^{2+} e_g orbital which polarizes the filled t_{2g} orbital. Therefore, the materials with higher degrees of disorder exhibit lower chemical shifts of lithium in the transition metal layer.

Comparing samples (c) and (d), the same trend is observed; chemical shifts of the more disordered sample (c) occur at lower frequency than the less disordered sample (d). The trend suggests a correlation between chemical shift and degree of cation disorder within mixed transition metal oxides, a concept which has not been previously demonstrated.

Evidence for Transition Metal Charge Ordering. Analysis of the spectra shows a decreasing degree of cation disorder for sample (d) that was slow-cooled, relative to the other samples that were quenched. This trend is logical, and although there is a small discrepancy with the degree of cation disorder determined by Rietveld analysis, it is self-consistent to detect the presence of transition metal charge ordering in the sample which exhibits the lowest degree of cation disorder according to the NMR line shape and chemical shift results. It is revealed by close examination of the main line shape of the ^{6}Li NMR spectrum for sample (d). The large hyperfine shifts, compared to the other samples, do support the lower cation disorder in sample (d) established by NMR. Moreover, the spectral decomposition for the central resonance of this spectrum (Figure 5) clearly

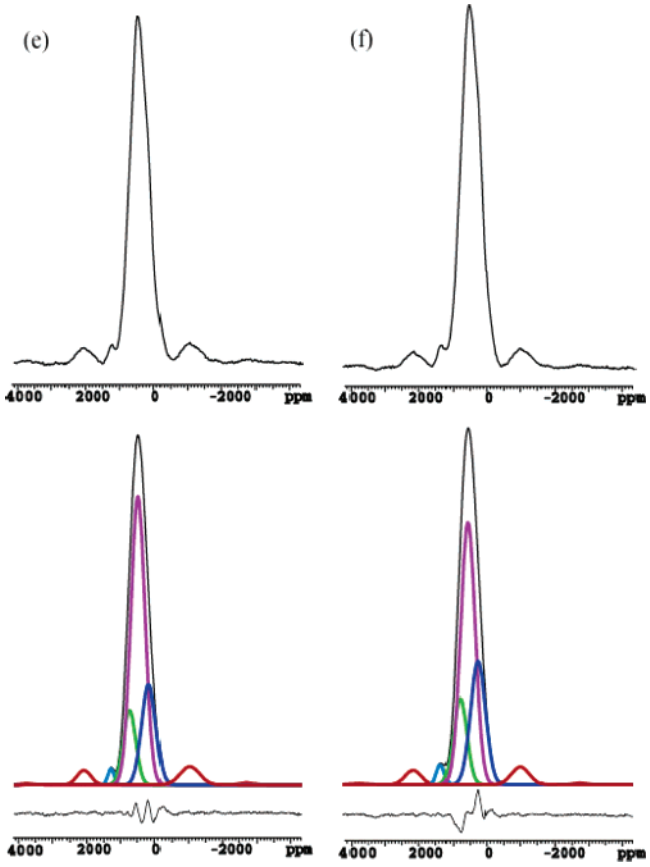

Figure 6. ^{6}Li MAS NMR spectra acquired at 29.7 MHz (4.7 T), under 46 kHz rotor spinning frequencies, in 1.8 mm rotors containing ~5 mg sample. Samples (e) and (f) were heated for 3 h at 1100 °C and quenched. The spinning sidebands are marked with an asterisk and the spectral decompositions are shown below the experimental data, with the fit in black. The residual difference between the fit and the experimental data is shown below the fit. Error estimates are based on the difference in peak area between repeated iterations of the spectral decomposition routine.

shows three distinct line shapes. These arise from the ordering of transition metal ions within the lithium local electronic environment. Sample (d) is unique, not only in the complexity of the line shape of ^{6}Li within the lithium oxide layers but also in that it was slow-cooled. We expect this to result in greater order within the sample.

To confirm this effect, two samples that were heated to 1100 °C were studied, which also show evidence of transition metal ordering in the main resonance. These spectra are shown in Figure 6e,f. Table 3 includes a summary of the decompositions, including chemical shifts and relative areas of the three line shapes that contribute to this main resonance. These two samples exhibit very low cation disorder determined by NMR, as expected due to the higher firing temperatures.[21] Also, the higher chemical shift for the Li environment in the transition metal layer (greater than 1300 ppm in both cases) follows the trend of expecting lower disorder values.

A driving force for ordering in these samples can be understood by considering local charge balance. According to Pauling's rule of electroneutrality, the sum of the electrovalencies of the nearest neighbor cations should equal

(21) Lu, Z. H.; Chen, Z. H.; Dahn, J. R. *Chem. Mater.* **2003**, *15*, 3214−3220.

Table 3. Summary of Decompositions of Samples Exhibiting Transition Metal Ordering

sample	chemical shift (ppm)	line width (kHz)	area ratio (highest frequency to lowest frequency)	% Li/Ni disorder by NMR	% Li/Ni disorder by XRD
(d) heated 3 h, 1000 °C, slow cooled	748	11.5	1:2:1	2.3	5.5
	519	10.3			
	236	10.2			
(e) heated 3 h, 1100 °C, quenched	756	13.1	1:4:1.3	1.4	4.8
	504	14.7			
	189	14.5			
(f) heated 3 h, 1100 °C, quenched	744	13.5	1:4:1.6	2.0	3.5
	520	15.0			
	220	15.5			

Table 4. Possible Local Coordination Environments for Li^+ Nuclei, Corresponding to Line Shape Decomposition Given in Figure 7 Based on the Pauling Electroneutrality Principle, and Propensity for $Ni^{2+}-Mn^{4+}$ Clustering

case	Ni^{2+}	Co^{3+}	Mn^{4+}	chemical shift
(a)	2	2	2	intermediate frequency
(b)	1	4	1	low frequency
(c)	3	0	3	high frequency

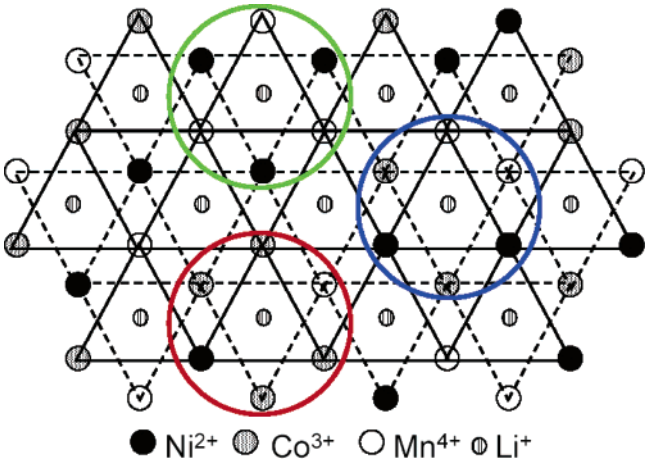

Figure 7. Proposed local charge ordering environments, based on the combination of environments described in Table 4. Case (a) is indicated by the blue circle, case (b) by the red circle, and case (c) by the green circle. Solid lines represent the top transition metal layer, and dotted lines represent the bottom transition metal layer. Despite the local ordering around the lithium nuclei, charge balance is maintained in both transition metal layers. The intervening lithium layer is shown as isolated atoms at the centers of the octahedron. Oxygen atoms are left out for simplicity.

the charge of the anion in ordered rock salt structures.[22] This method has been used to understand local short-range ordering in Li_2MnO_3 and the potential cathode material $Li_{1.2}Cr_{0.4}Mn_{0.4}O_2$.[23] Li_2MnO_3 is the classic example of a material which long-range orders because of electroneutrality and is identified through X-ray diffraction as a $\sqrt{3}a_{hex} \times \sqrt{3}a_{hex}$ superlattice according to Wood's notation.[24]

In $Li[Ni_{1/3}Mn_{1/3}Co_{1/3}]O_2$ there are three different ways to distribute the transition metal cations around the lithium nucleus that satisfy Pauling's rule by preserving local electroneutrality around oxygen. These cases are summarized in Table 4 and illustrated in Figure 7. Case (a), where Ni^{2+}, Co^{3+}, and Mn^{4+} are evenly arranged around the Li atom, describes a scenario that would result in only one chemical shift in the NMR. If the array were organized to give long-range order, one single narrow line shape would result. Any perturbation of the possible $Ni^{2+}/Co^{3+}/Mn^{4+}$ arrangements around the Li center would simply result in an equivalent shift but a broader line. Cases (b) and (c), on the other hand, represent uneven distributions that would exhibit different chemical shifts.

These three types of possible environments correspond to the three line shapes present in the decomposition spectrum for the sample which showed the smallest cation disorder by NMR. Ni^{2+} and Mn^{4+} both transfer positive spin density via the delocalization mechanism with the Li 2s orbital, 180° and 90°, respectively. Following this model, case (b) is dominated by diamagnetic Co^{3+} and is therefore assigned to the shift at lower frequency while case (c) is attributable to the resonance at highest frequency. The area of these outer peaks is roughly equal, suggesting that there is a similar distribution of each coordination environment throughout the lattice. This assignment is supported by several factors. Considering all three possible arrangements, the total number of ions of each type is the same for all three metals, corresponding to the experimentally determined stoichiometry. As well, strong interactions between Ni^{2+} and Mn^{4+} ions have been shown to be favorable by first-principle calculations which supports the fact that the greater number of Mn^{4+} ions in case (c) is accompanied by a greater number of Ni^{2+} ions.[9,11]

The "very local" nonrandom distributions of the different transition metal ion environments described above could extend to the formation of clusters or domains. The appearance of domains within mixed transition metal oxides have been observed using solid-state MAS NMR for solid solutions of the form $LiNi_{1-y}Co_yO_2$[25] and $Li[Li_yCr_xMn_{1-x-y}]O_2$[15] and by electron diffraction in $Li[Ni_xLi_{1/3-2x/3}Mn_{2/3-x/3}]O_2$.[26] A model of the local transition metal ordering in $Li[Ni_{1/3}Mn_{1/3}Co_{1/3}]O_2$ is shown in Figure 7. Hypothetically, if these cation domains reached a critical size, they could become detectable by techniques such as neutron diffraction (PND) that are sensitive to long-range ordering. Our PND experiments on these materials indicate this limit is not reached, however, as no superlattice formation was observed. We note that the degree of disorder and the existence of short- and long-range ordering are strongly dependent on the synthetic

(22) Mather, G. C.; Dussarrat, C.; Etourneau, J.; West, A. R. *J. Mater. Chem.* **2000**, *10*, 2219−2230.
(23) Ammundsen, B.; Paulsen, J.; Davidson, I.; Liu, R. S.; Shen, C. H.; Chen, J. M.; Jang, L. Y.; Lee, J. F. *J. Electrochem. Soc.* **2002**, *149*, A431−A436.
(24) Strobel, P.; Lambertandron, B. *J. Solid State Chem.* **1988**, *75*, 90−98.
(25) Marichal, C.; Hirschinger, J.; Granger, P.; Menetrier, M.; Rougier, A.; Delmas, C. *Inorg. Chem.* **1995**, *34*, 1773−1778.
(26) Meng, Y. S.; Ceder, G.; Grey, C. P.; Yoon, W. S.; Jiang, M.; Breger, J.; Shao-Horn, Y. *Chem. Mater.* **2005**, *17*, 2386−2394.

conditions.[20,21] In particular, slow cooling and higher firing temperatures seem to minimize disorder and in turn minimize irreversible capacity.[5] In terms of preparation conditions, sample (d), being heated at a high temperature for a long time and slow-cooled, favors the low degree of Li^+/Ni^{2+} cation disorder determined by NMR. Similarly, samples (e) and (f), which were heated to 1100 °C, also exhibited lower cation disorder.

It is interesting to note that long-range ordering of the transition metal ions in $Li[Ni_{1/3}Mn_{1/3}Co_{1/3}]O_2$ was originally proposed by Ohzuku et al., based on calculations of the formation energy.[27,28] Their suggested $\sqrt{3}a_{hex} \times \sqrt{3}a_{hex}$ $P3_112$ superlattice consists of a single transition metal coordination around the Li nucleus, equally ordered with $2Co^{3+}-2Ni^{2+}-2Mn^{4+}$ transition metal neighbors.[28] This corresponds to the long-range ordered extreme of case (a) above. Observation of such a superlattice would likely be highly sample preparation-dependent, and the ordering could range over different domain sizes. The model presented here (Figure 7) differs in that the local ordering we propose is intermediate. It is dominated by a random distribution of two of each of the transition metal ions (case (a)) but includes contributions from the two less random cases ((b) and (c)). Like long-range ordering, the local ordering model maintains charge neutrality, but allows for the preferred association of nickel and manganese ions. It also explains why, to date, X-ray and neutron diffraction have failed to provide clear evidence of the former.[7,29,30] Finally, the observation of even local transition metal charge ordering is dependent on a low degree of Li^+ cation disorder, as high degrees of Li^+/Ni^{2+} exchange would alter the charge distribution within the metal layers.

Conclusions

In summary, solid-state ^{6}Li NMR has been shown to be a reliable method for determining the degree of cation disorder within cathode materials, when compared to diffraction studies combined with Rietveld refinement. This paper presents the first evidence of local transition metal charge ordering seen by any experimental technique for the $Li[Ni_{1/3}Mn_{1/3}Co_{1/3}]O_2$ compound and should provide further insight into the relationship between structural properties and electrochemical performance in such materials. This local ordering of the transition metal ions is an intermediate scenario, between the full superstructure and a completely random organization of the transition metal layers. This indicates that, in these materials, the observed $Ni^{2+}-Mn^{4+}$ association is only a weak thermodynamic driving force and does not result in a complete structural organization, even under carefully controlled synthetic conditions. The evidence for charge ordering within the slow-cooled sample suggests the possibility that this material may form a restricted superstructure and it may display superior electrochemical behavior. These studies of the electrochemical performance of these materials and related materials of differing preparation methods are ongoing.

Furthermore, we have shown a correlation between the degree of cation disorder in a given sample and the magnitude of the NMR chemical shifts. While this effect may be unique to the $^1/_3$ $^1/_3$ $^1/_3$ class of materials, it will be interesting to see whether it can be established in related materials.

Acknowledgment. The authors are grateful to the scientists at INCO, including Dr. Feng and Dr. Quan, for interesting discussions and providing precursor materials. We thank Ian Swainson at the Chalk River Neutron Facility (Chalk River, Canada) for acquiring the neutron diffraction data. Also, L.F.N. and G.R.G. independently acknowledge the financial support of NSERC through individual Strategic and Discovery Grants and also INCO, and Manufacturing Materials Ontario (MMO) through an EMK-MMO collaborative grant. A.S. would like to acknowledge funding from the Estonian Science Foundation.

CM0508773

(27) Koyama, Y.; Tanaka, I.; Adachi, H.; Makimura, Y.; Ohzuku, T. *J. Power Sources* **2003**, *119*, 644−648.
(28) Koyama, Y.; Yabuuchi, N.; Tanaka, I.; Adachi, H.; Ohzuku, T. *J. Electrochem. Soc.* **2004**, *151*, A1545−A1551.
(29) Yabuuchi, N.; Koyama, Y.; Nakayama, N.; Ohzuku, T. *J. Electrochem. Soc.* **2005**, *152*, A1434−A1440. Note added in proof: this paper appeared after our submission and suggests the presence of a $P3_112$ superlattice, but still with short-range order as seen by electron diffraction, and consistent with our findings.
(30) Whitfield, P. S.; Davidson, I. J.; Cranswick, L. M. D.; Swainson, I. P.; Stephens, P. W. *Solid State Ionics* **2005**, *176*, 463−471.